

## Electronic Supplementary Information

### New Challenge of Metal-Organic Frameworks for High-Efficient Separation of Hydrogen Chloride toward Clean Hydrogen Energy

Jia Liu,<sup>a,c</sup> Wei Xia,<sup>a</sup> Weijun Mu,<sup>a,c</sup> Peizhou Li,<sup>b,c</sup> Yanli Zhao,<sup>b,c,\*</sup> Ruqiang Zou<sup>a,c,\*</sup>

<sup>a</sup> Department of Materials Science and Engineering, College of Engineering, Peking University, Beijing 100871, China. Email: rzou@pku.edu.cn

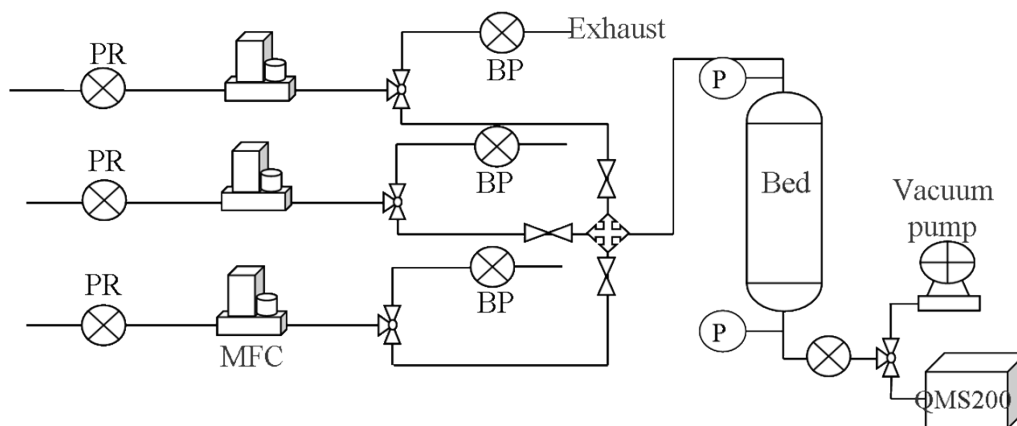
<sup>b</sup> Division of Chemistry and Biological Chemistry, School of Physical and Mathematical Sciences, Nanyang Technological University, 21 Nanyang Link, Singapore 637371, Singapore. E-mail: zhaoyanli@ntu.edu.sg.

<sup>c</sup> Singapore Peking University Research Centre for a Sustainable Low-Carbon Future, 1 Create Way, Singapore 138602.

#### Breakthrough Testing

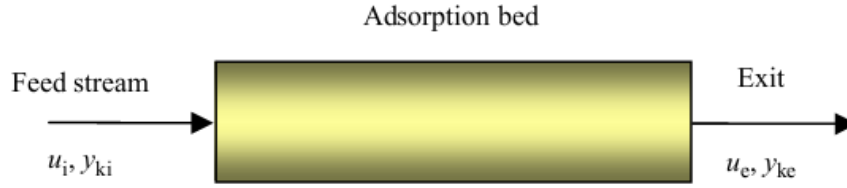
A schematic representation of the breakthrough test system is shown in Figure S1. The mass flow controllers (MFC) of precision  $\pm 1\%$  (purchased from Beijing Seven star Electronics Co. Ltd) were used to control the flow rates in the two passages of the adsorber: one passage for the mixture gas, the other for the carrier gas (helium). A back-pressure regulator was used to control the pressure of the adsorption. Pressure was measured by using pressure transmitters purchased with accuracy  $\pm 0.1\%$ . The test temperature was kept constant within  $\pm 0.1$  °C by using a thermostat.

All the breakthrough tests were carried out at a temperature of 25°C. Each sample was packed in a stainless tube with length of 8cm and inner diameter of 4 mm. All samples were purged with purity helium for 20 min at 200 °C at the beginning. The outlet gases were detected by using a QMS 200 mass spectrometer with a sampled rate of 1 point per second. The concentration of the outlet gas was calibrated by comparing it to the concentration of the source gas recorded by the mass spectrometer under the same flow rate.



**Scheme S1.** Schematic diagram of the setup to collect breakthrough curves. PR: pressure regulator; MFC: mass flow controller; BP: back pressure regulator; P: pressure transducer; QMS: quadrupole mass spectrograph.

## Calculations



**Scheme S2.** Mass balance over the adsorption bed.

As shown in Scheme S2, the composition of inlet gas was constant, but the outlet gas composition was a function of time for a definite period and the breakthrough curve was thus formed. The uptake and selectivity of gases were evaluated on the basis of breakthrough curves:

$$n_k = \frac{(\int_0^t u_i y_{k,i} dt - \int_0^t u_e y_{k,e} dt) AC - \varepsilon AL y_{k,i} p / RT}{m} \quad (1)$$

where  $u_i$  and  $u_e$  are the linear speeds of flow at the entrance and exit of the adsorption bed, respectively;  $A$  and  $L$  are the section area and length of the adsorption bed;  $C$  is the total concentration of the gas stream;  $y_{k,i}$  and  $y_{k,e}$  are the concentration of component  $k$  in the gas stream at the entrance and exit of the adsorption bed, respectively;  $\varepsilon$  is the fractional void of the adsorption bed and can be evaluated in the volumetric setup of adsorption measurement;  $m$  is the mass of adsorbent. The result of integration was calculated by using origin software according to mass spectrograph.

The separation coefficient of adsorption is defined as:

$$Selectivity = \frac{n_j}{n_i} \times \frac{x_i}{x_j} \quad (2)$$

where  $x$  and  $y$  are the molar fractions of components  $i$  and  $j$  in the adsorbed phase and the gas phase at equilibrium, respectively.

For example, the selectivity of HCl on UiO-66 at 298K was calculated by its breakthrough curve (Fig. S34). Uptake was obtained from equation 1. Flow rate is 67 mL/min, void volume is about 32.01 mL, test temperature is 298 K, and sample mass is 0.529g.

$$\begin{aligned} HCl_{uptake} &= \frac{(26.92 \text{ min} \times 67 \text{ ml} / \text{min} \times 10\% - 90.832 \text{ ml} - 32.01 \text{ ml} \times (273.15 \text{ K} / 298 \text{ K}) \times 10\%)}{0.529 \text{ g} \times 22.4 \text{ ml} / \text{mmol}} \\ &= 7.31 \text{ mmol/g} \end{aligned}$$

$$\begin{aligned} H_2_{uptake} &= \frac{(26.92 \text{ min} \times 67 \text{ ml} / \text{min} \times 10\% - 177.3337 \text{ ml} - 32.01 \text{ ml} \times (273.15 \text{ K} / 298 \text{ K}) \times 10\%)}{0.529 \text{ g} \times 22.4 \text{ ml} / \text{mmol}} \\ &= 0.00833 \text{ mmol/g} \end{aligned}$$

$$Selectivity = \frac{7.31 \text{ mmol} / \text{g}}{0.008334 \text{ mmol} / \text{g}} \times \frac{10\%}{10\%} = 877$$

## Simulations

Grand canonical Monte Carlo simulations were used to calculate HCl adsorption on Mil-101(Cr) and UiO-66. In the simulations, the MOFs structure was assumed to be rigid, because the experimental results show that it was no change before and after adsorption of HCl. In each simulation, the atom position was taken from reported MIL-101(Cr) and (UiO-66),<sup>1</sup> the box consisted of  $2 \times 2 \times 2$  unit cells representing UiO-66 and  $1 \times 1 \times 1$  unit cells representing MIL-101(Cr), cut off radius for the force field of 20 Å was used, and periodic boundary conditions were applied in every direction. In the grand

canonical ensemble, the chemical potential of each component, the temperature and the volume were fixed. Numbers of molecules were then allowed to fluctuate until the required chemical potential was attained. The Lennard-Jones parameters for the structures were taken from the compass, and UFF force field and the coulombic interactions were calculated using Ewald summation technique.<sup>2-4</sup>

## References

- 1 A. Schaate, P. Roy, A. Godt, J. Lippke, F. Waltz, M. Wiebcke and P. Behrens, *Chem. Eur. J.* 2011, **17**, 6643-6651.
- 2 Y. Zeng, X. Zhu, Y. Yuan, X. Zhang and S. Ju, *Sep. Purif. Technol.* 2012, **95**, 149-156.
- 3 B. Supronowicz, A. Mavrandonakis and T. Heine, *J. Phys. Chem. C* 2013, **117**, 14570-14578.
- 4 L. Hamon, H. Leclerc, A. Ghoufi, L. Oliviero, A. Travert, J.-C. Lavalley, T. Devic, C. Serre, G. r. Férey, G. De Weireld, A. Vimont and G. Maurin, *J. Phys. Chem. C* 2011, **115**, 2047-2056.

## Synthesis

- 1 MIL-101(Cr): The synthesis of MIL-101(Cr) consists of hydrothermal reaction of H<sub>2</sub>BDC (166 mg at 1 mmol) with Cr(NO<sub>3</sub>)<sub>3</sub>•9H<sub>2</sub>O (400 mg at 1 mmol), fluorhydric acid (0.2 mL at 1 mmol), and H<sub>2</sub>O (4.8 mL at 265 mmol) for 8 hours at 220 °C.<sup>1</sup>
- 2 MOF-5: Zn(NO<sub>3</sub>)<sub>2</sub>•6H<sub>2</sub>O (7.18 g) and H<sub>2</sub>BDC (1.33 g) were dissolved into DMF solution (200 mL). The mixture was treated under 60 °C for 3 days. After filtration, the obtained liquid was added with hexadecyl trimethyl ammonium bromide (CTAB, 10 g) under stirring for 30 min. Adding triethylamine (7.5 mL) into the mixture yielded colorless fine powder that was formulated as Zn(BDC)(DMF)(H<sub>2</sub>O).<sup>2</sup>
- 3 CuBTC: CuBTC (HKUST-1) was prepared by solvothermal method. Benzene-1,3,5-tricarboxylic acid (5.0g, 24 mmol) and copper(II) nitrate hemipentahydrate (10.0 g, 43 mmol) were stirred for 15 min in solvent (250 mL) consisting of DMF, ethanol and deionized water (1:1:1) in a 1 L glass jar. The jar was tightly capped and placed in oven at 85°C for 20 hour. After rinsing with DMF, the product was soaked in dichloromethane for 3 days with replenishing three times. The product was obtained after removal of solvent under vacuum at 170 °C for 8 h.<sup>3</sup>
- 4 ZIF-8: ZIF-8 was synthesized in a purely aqueous system. Firstly, Zn(NO<sub>3</sub>)<sub>2</sub>•6H<sub>2</sub>O (1.17 g) was dissolved in deionized water (8 g). Secondly, 2-methylimidazole (22.70 g) was dissolved in another deionized water (80 g). The two solutions were mixed under stirring at room temperature. The synthesis solution turned milky almost instantly after the two solutions were mixed. After stirring for 5 min, the product was collected by centrifugation, which was then washed with deionized water for several times. The product was dried at 65 °C overnight in vacuum.<sup>4</sup>
- 5 [Cu(bdc)(TED)<sub>0.5</sub>]•2DMF: A mixture of copper(II) nitrate trihydrate (740 mg), terephthalic acid (680 mg) and triethylenediamine (480 mg) in DMF (150 mL) was heated at 100°C for 36 hours. The blue Powder was obtained after filtering, rinsing with DMF and drying under vacuum.<sup>5</sup>
- 6 UiO-66 and UiO-66(NH<sub>2</sub>): ZrCl<sub>4</sub> (0.080g, 0.343mmol for UiO-66; 0.062g, 0.343mmol for UiO-66(NH<sub>2</sub>)) and 30 equivalents of modulator (0.588mL, 10.29mmol of acetic acid) were dissolved in DMF (20 mL) by using ultrasound for 10 minutes. The linker was added to the clear solution in an equimolar ratio with regard to ZrCl<sub>4</sub> (0.056g, 0.343mmol for Zr-BDC) and dispersed by ultrasound for about 10 minutes until it was completely dissolved. The resulting mixture was placed in a preheated oven at 120°C for 24 h. After the solution was cooled to room temperature, the solid was filtered. The particles that obtained were denoted as “as-synthesized”. The precipitates were immersed in DMF (20mL) for 5 h and then were centrifuged and washed with ethanol (10mL). After this procedure, the desired materials were obtained.<sup>6,7</sup>
- 7 MOF-74: A mixture of 2,5-dihydroxy-1,4-benzenedicarboxylic acid (H<sub>2</sub>-DHBDC) (0.096mmol) and Mg(NO<sub>3</sub>)<sub>2</sub>•4(H<sub>2</sub>O) (0.203mmol) was dissolved in a mixture solution of DMF (2.0 mL), 2-propanol (0.1 mL) and water (0.1 mL), which was placed in a Pyrex tube frozen in a liquid nitrogen

bath. The tube was evacuated and flame-sealed, then heated to 105 °C for 20 h. After cooling to room temperature, the yellow crystals were produced, which were dried in air after washing with DMF and ethanol.<sup>8</sup>

8 Fe-BTC gel: Fe(NO<sub>3</sub>)<sub>3</sub>•6H<sub>2</sub>O and H<sub>3</sub>BTC were dissolved in ethanol (30mL) respectively at room temperature. The solutions were mixed and stirred quickly until the gel solid was observed. The sample was kept in room temperature for one hour, and dried by CO<sub>2</sub> drying process.<sup>9</sup>

9 Al-BTC gel: Al(NO<sub>3</sub>)<sub>3</sub>•9H<sub>2</sub>O (0.015 mol) and H<sub>3</sub>BTC (0.01 mol) were added to ethanol (70 mL). The mixture was stirred at room temperature for 15 min to dissolve the solid. Then, the transparent liquid was transferred to a sealed container, which was heated to 120 °C. After one hour, a light yellow integrated gel monolith was formed. The resulting wet gel was air dried for a few hours to remove the solvent or dried in an oven at a low temperature to accelerate this process. After the drying step, the gel shrunk and turned into xerogel particles. An aerogel sample was prepared from the wet gel through a supercritical CO<sub>2</sub> drying process.<sup>10</sup>

10 Y-BTC: Y-BTC was synthesized by dissolving Y(NO<sub>3</sub>)<sub>3</sub>•6H<sub>2</sub>O (3.677 g, 9.6 mmol) and 1,3,5-benzenetricarboxylic acid (1.681 g, 8.0 mmol) in a mixture solvent of DMF (50 mL) and deionized water (10mL) at room temperature in a volumetric flask. The mixture was stirred with dripping 8 drops of triethylamine and 3 drops of nitric acid successively. The resulting mixture was sealed and placed in an oven at 100 °C for 17 hours. After the solution was cooled to room temperature, the resulting solid was filtered and repeatedly washed with absolute ethanol for 3 times. The white powder was filtered, and then dried under vacuum at ambient temperature.<sup>11</sup>

## References

- 1 G. Férey, C. Mellot-Draznieks, C. Serre, F. Millange, J. Dutour, S. Surblé and I. Margiolaki, *Science* 2005, **309**, 2040-2042.
- 2 H. Li, M. Eddaoudi, M. O'Keeffe and O. M. Yaghi, *Nature* 1999, **402**, 276-279.
- 3 A. Vishnyakov, P. I. Ravikovitch, A. V. Neimark, M. Bülow and Q. M. Wang, *Nano Lett.* 2003, **3**, 713-718.
- 4 H. Hayashi, A. P. Cote, H. Furukawa, M. O'Keeffe and O. M. Yaghi, *Nat. Mater.* 2007, **6**, 501-506.
- 5 K. Tan, N. Nijem, P. Canepa, Q. Gong, J. Li, T. Thonhauser and Y. J. Chabal, *Chem. Mater.* 2012, **24**, 3153-3167.
- 6 F. Vermoortele, R. Ameloot, A. Vimont, C. Serre and D. De Vos, *Chem. Commun.* 2011, **47**, 1521-1523.
- 7 J. H. Cavka, S. Jakobsen, U. Olsbye, N. Guillou, C. Lamberti, S. Bordiga and K. P. Lillerud, *J. Am. Chem. Soc.* 2008, **130**, 13850-13851.
- 8 N. L. Rosi, J. Kim, M. Eddaoudi, B. Chen, M. O'Keeffe and O. M. Yaghi, *J. Am. Chem. Soc.* 2005, **127**, 1504-1518.
- 9 P. Horcajada, S. Surble, C. Serre, D.-Y. Hong, Y.-K. Seo, J.-S. Chang, J.-M. Greneche, I. Margiolaki and G. Férey, *Chem. Commun.* 2007, 2820-2822.
- 10 C. Volkringer, D. Popov, T. Loiseau, G. Férey, M. Burghammer, C. Riekel, M. Haouas and F. Taulelle, *Chem. Mater.* 2009, **21**, 5695-5697.
- 11 O. M. Yaghi, H. Li and T. L. Groy, *J. Am. Chem. Soc.* 1996, **118**, 9096-9101

**Table S1.** Uptake of 11 MOFs in cycling experiments under the HCl partial pressure of 0.1 bar at 298 K.

	cycle 1 uptake mmol/g	cycle 2 uptake mmol/g	cycle 3 uptake mmol/g	cycle 4 uptake mmol/g	cycle 5 uptake mmol/g	cycle 6 uptake mmol/g
Fe-BTC	11.78	0	-	-	-	-
Cu-BDC(ted) <sub>0.5</sub>	10.86	0	-	-	-	-
UiO-66(NH <sub>2</sub> )	9.78	7.23	-	-	-	-
Mg-MOF-74	9.22	0	-	-	-	-
MIL-101(Cr)	7.67	7.67	7.63	7.64	7.65	7.64
UiO-66	7.31	7.28	7.29	7.30	7.27	7.28
MOF-5	6.44	0	-	-	-	-
Cu-BTC	4.98	0	-	-	-	-
Al-BTC	3.42	0	-	-	-	-
ZIF-8	2.89	0	-	-	-	-
Y-BTC	1.24	0	-	-	-	-

**Table S2.** Selectivity of 11 MOFs in cycling experiments under the HCl partial pressure of 0.1 bar at 298 K.

	cycle 1	cycle 2	cycle 3	cycle 4	cycle 5	cycle 6
Fe-BTC	4846	-	-	-	-	-
Cu-BDC(ted) <sub>0.5</sub>	2618	-	-	-	-	-
UiO-66(NH <sub>2</sub> )	1484	869	-	-	-	-
Mg-MOF-74	1514	-	-	-	-	-
MIL-101(Cr)	1363	1378	1398	1374	1387	1365
UiO-66	877	886	897	905	878	889
MOF-5	872	-	-	-	-	-
Cu-BTC	812	-	-	-	-	-
Al-BTC	704	-	-	-	-	-
ZIF-8	2367	-	-	-	-	-
Y-BTC	132	-	-	-	-	-

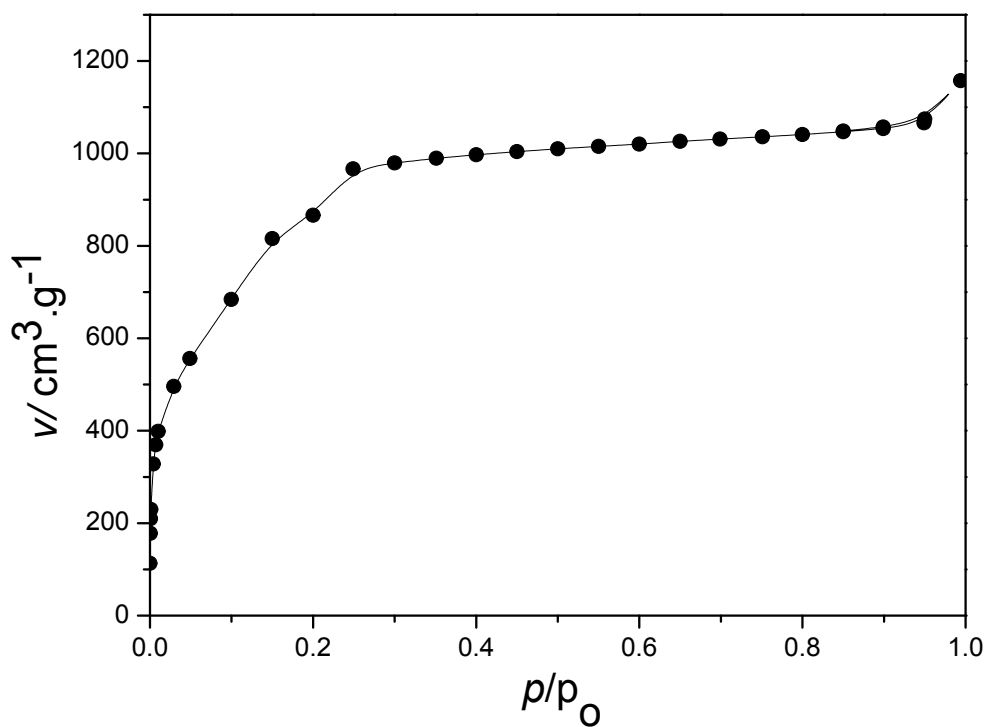


**Figure S1.** N<sub>2</sub> isotherm of MIL-101(Cr) at 77 K.

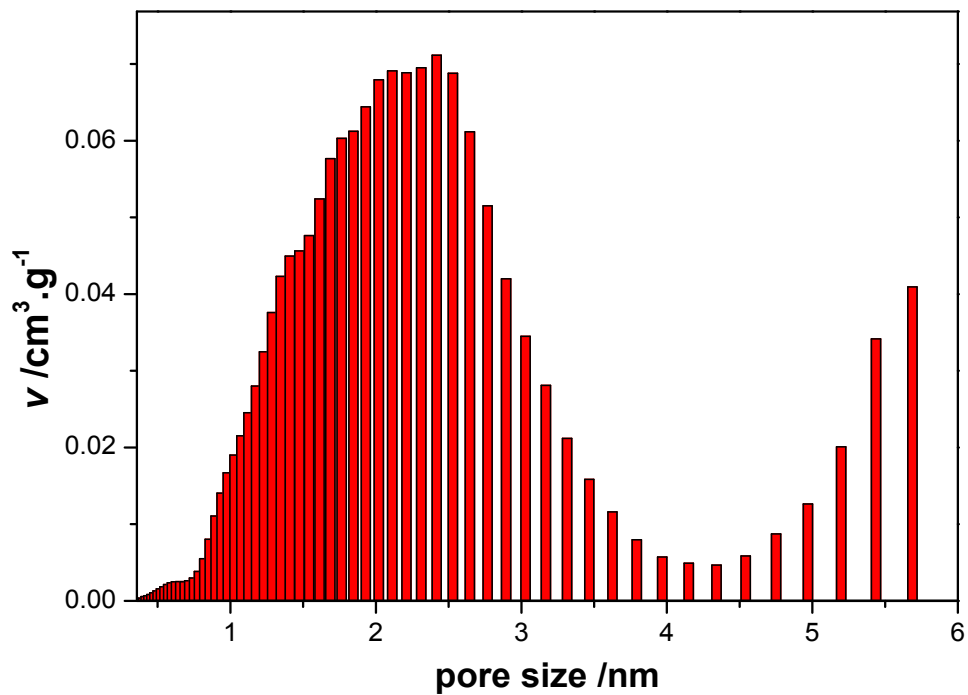


**Figure S2.** DFT pore size distribution of MIL-101(Cr).

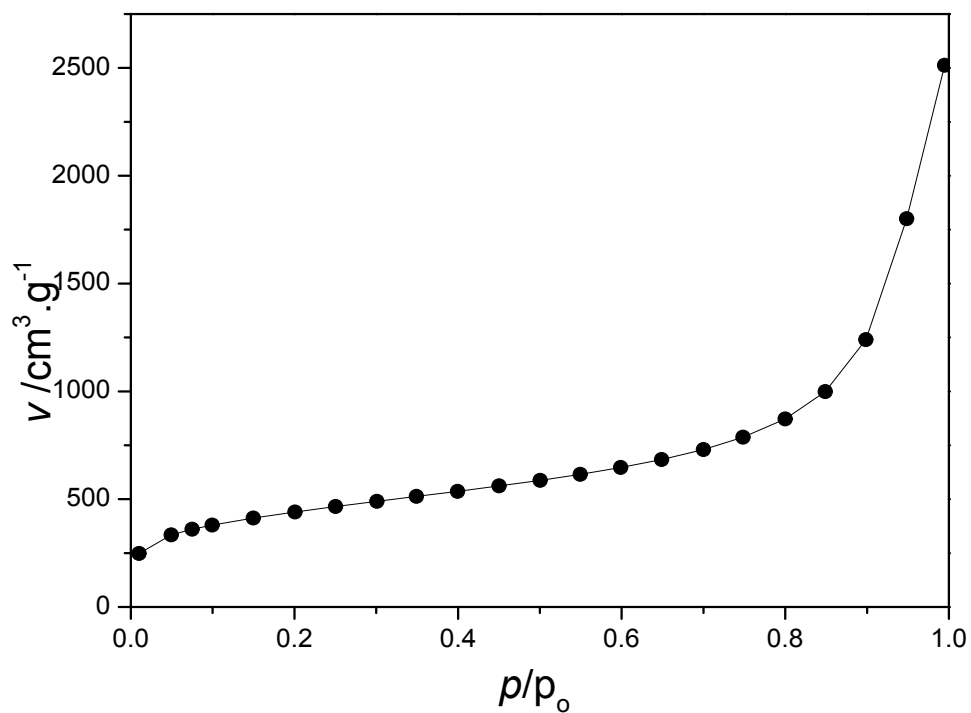


**Figure S3.** N<sub>2</sub> isotherm of Al-BTC gel at 77 K.

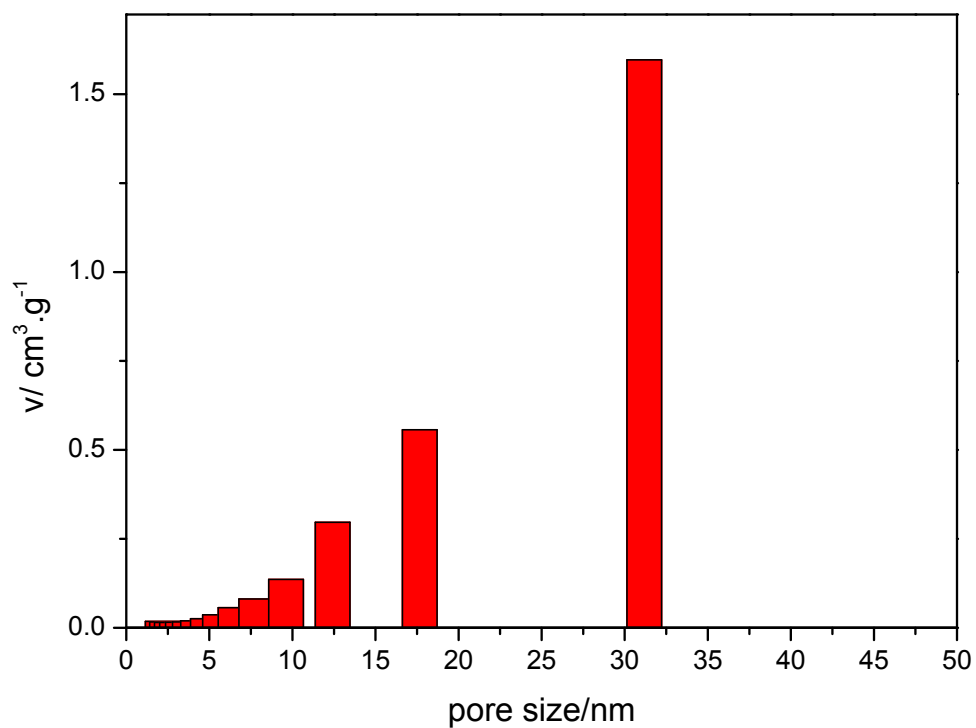


**Figure S4.** BJH pore size distribution of Al-BTC gel.

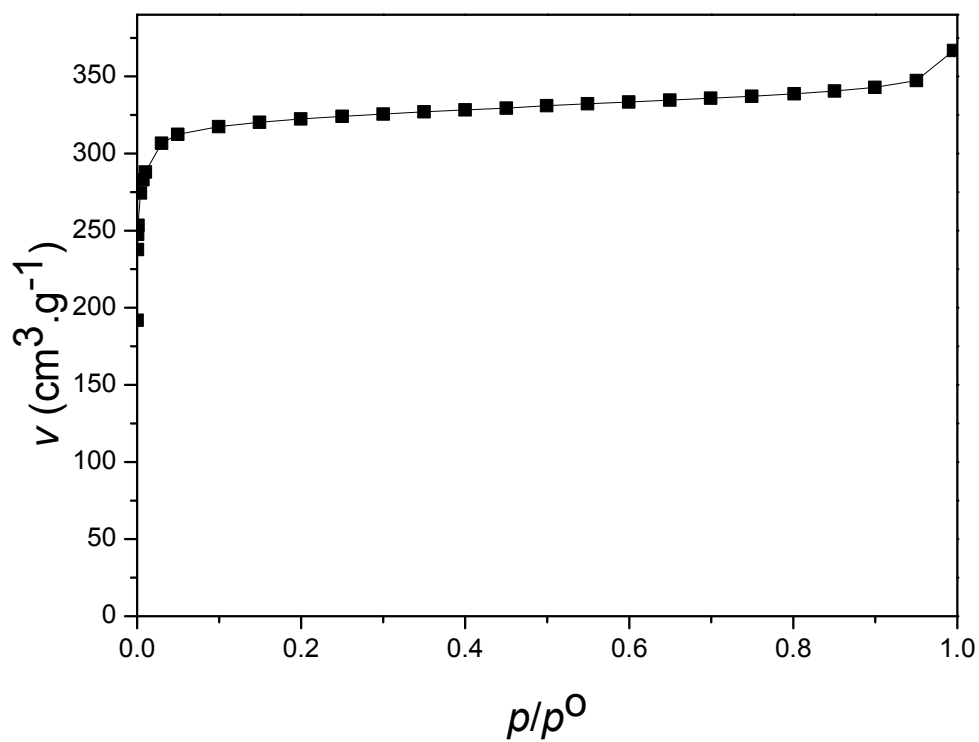


**Figure S5.** N<sub>2</sub> isotherm of UiO-66 at 77K.

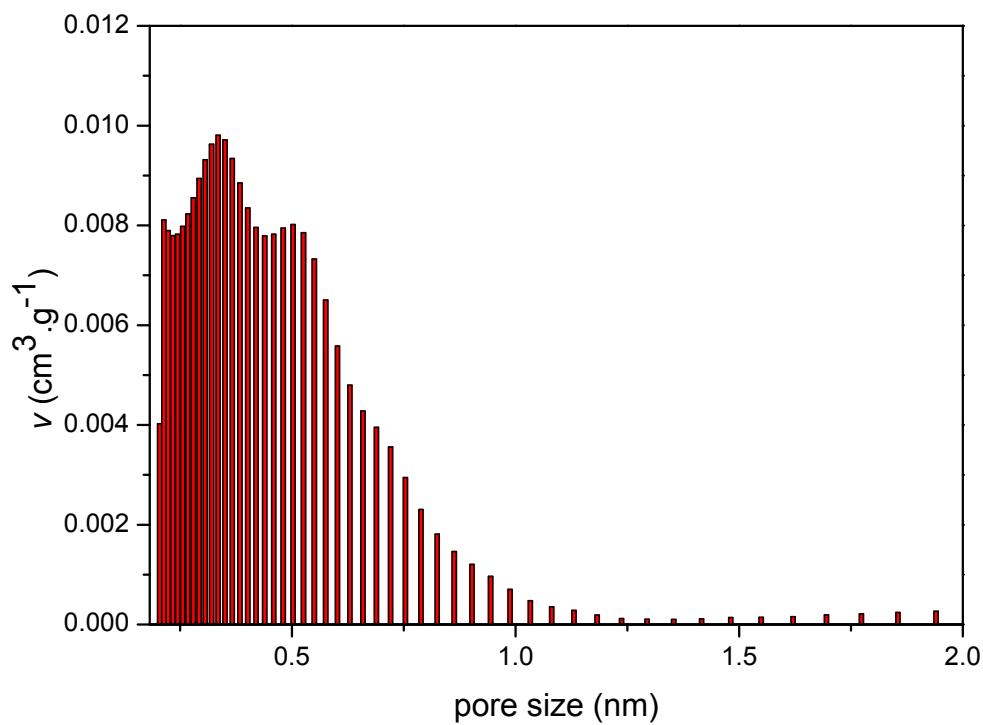


**Figure S6.** DFT pore size distribution of UiO-66.



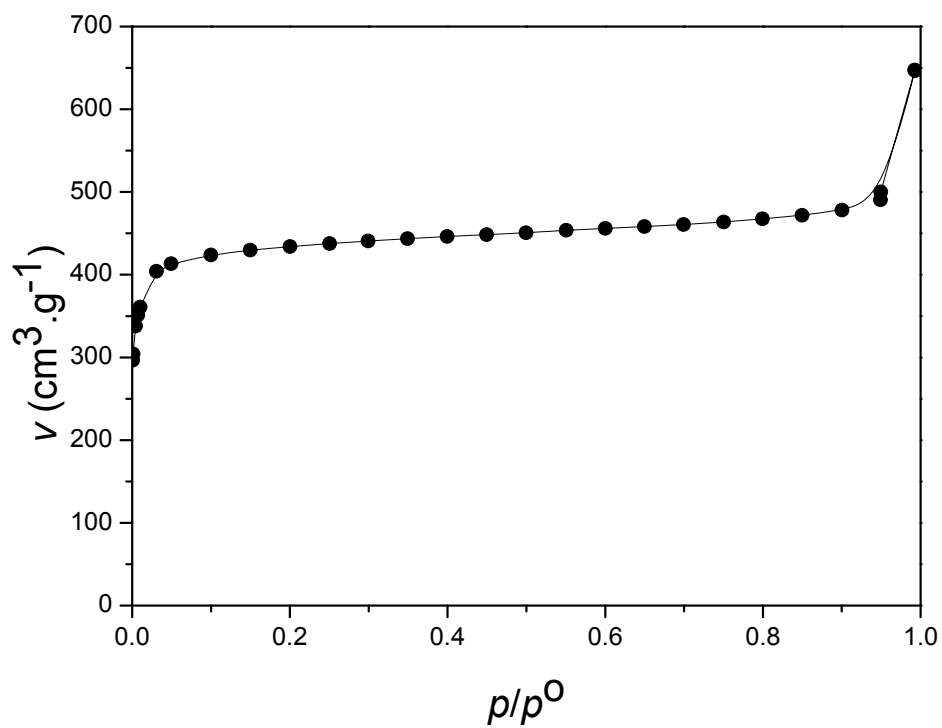


**Figure S7.** N<sub>2</sub> isotherm of UiO-66(NH<sub>2</sub>) at 77K.

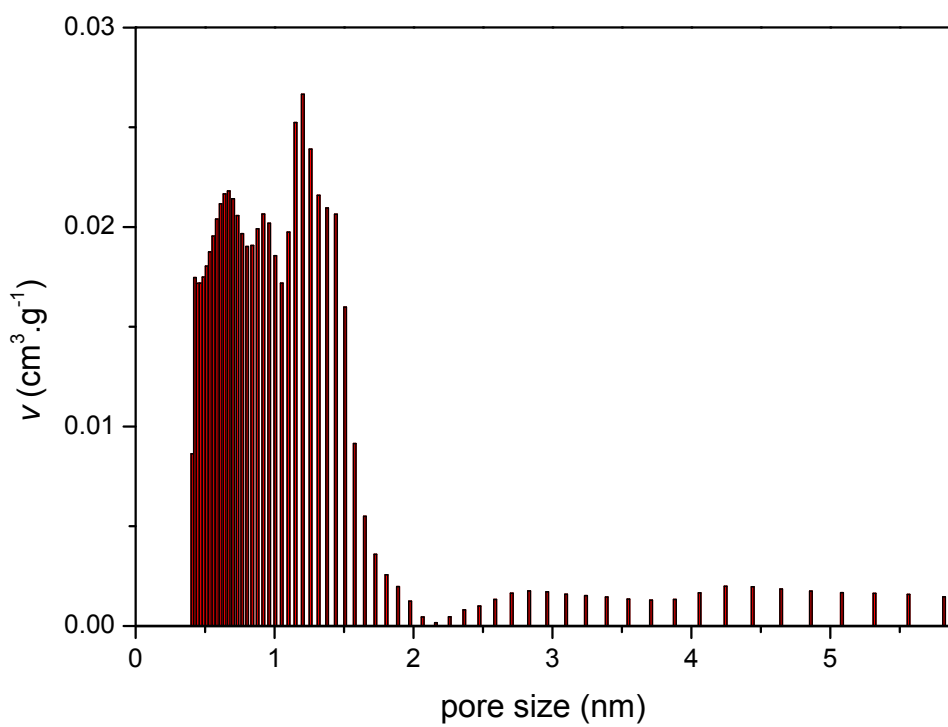


**Figure S8.** DFT pore size distribution of UIO-66(NH<sub>2</sub>).

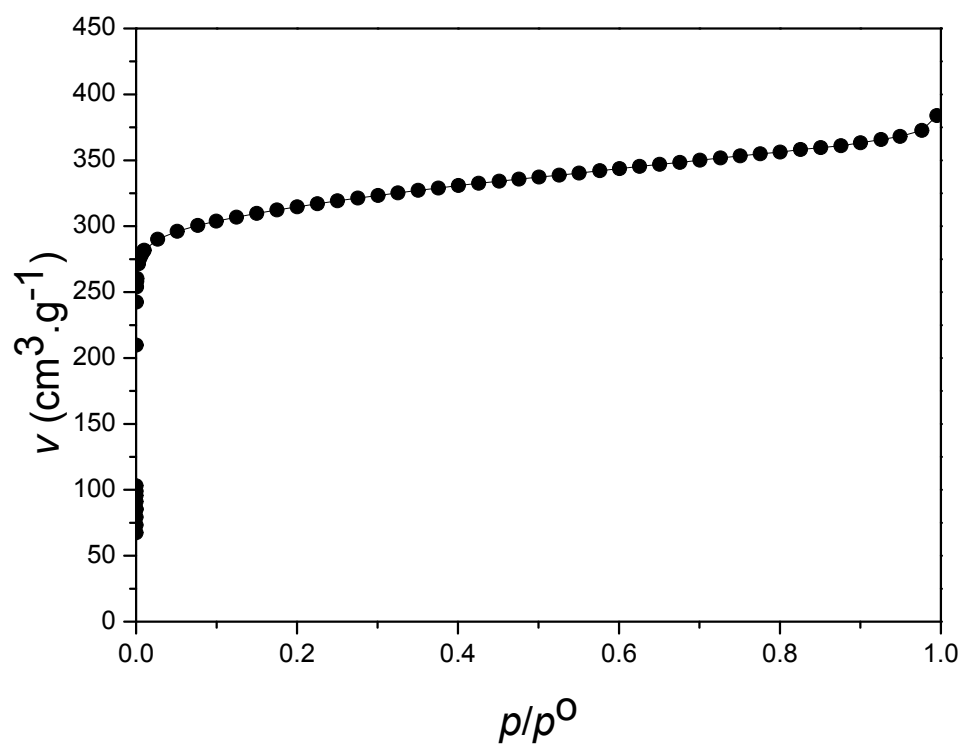


**Figure S9.**  $\text{N}_2$  isotherm of Cu-BDC(TED) at 77K.

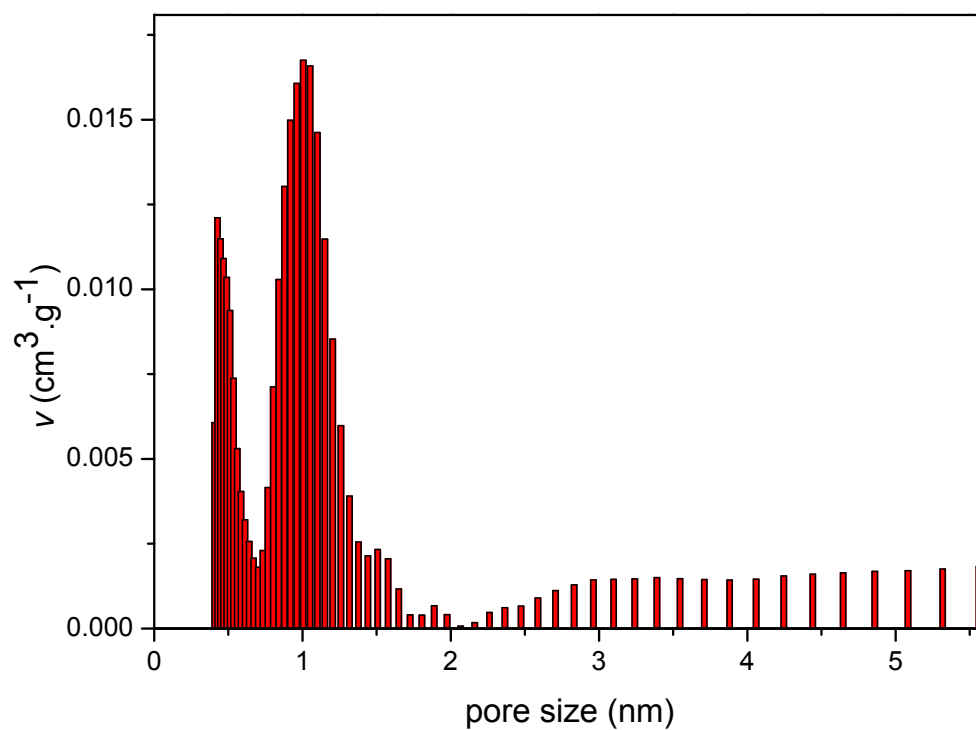


**Figure S10.** DFT pore size distribution of Cu-BDC(TED).

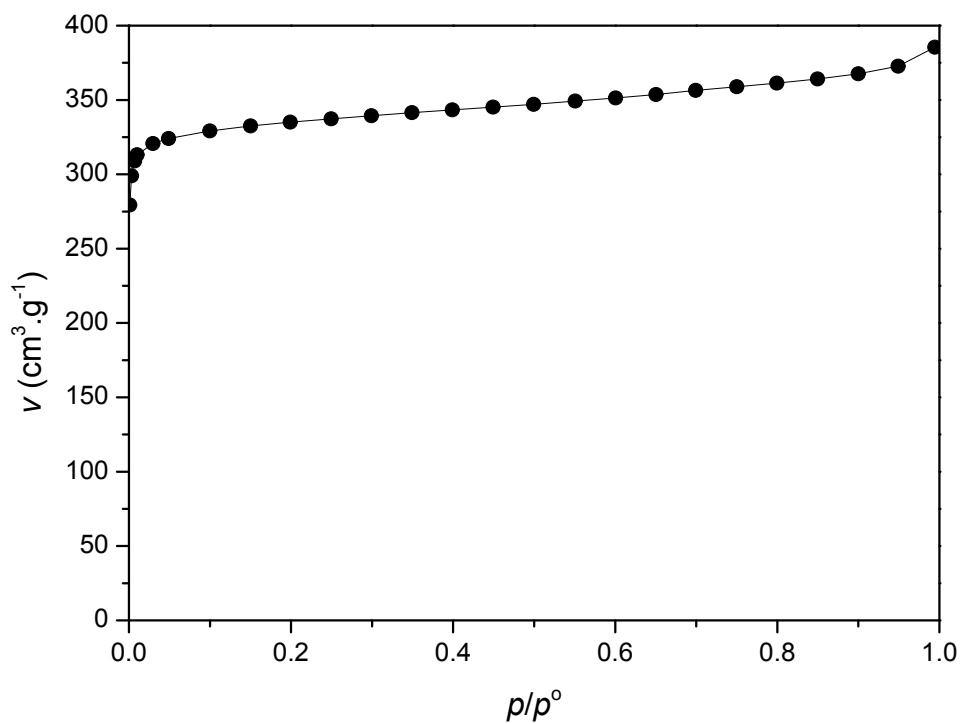


**Figure S11.**  $\text{N}_2$  isotherm of MOF-74 at 77K.

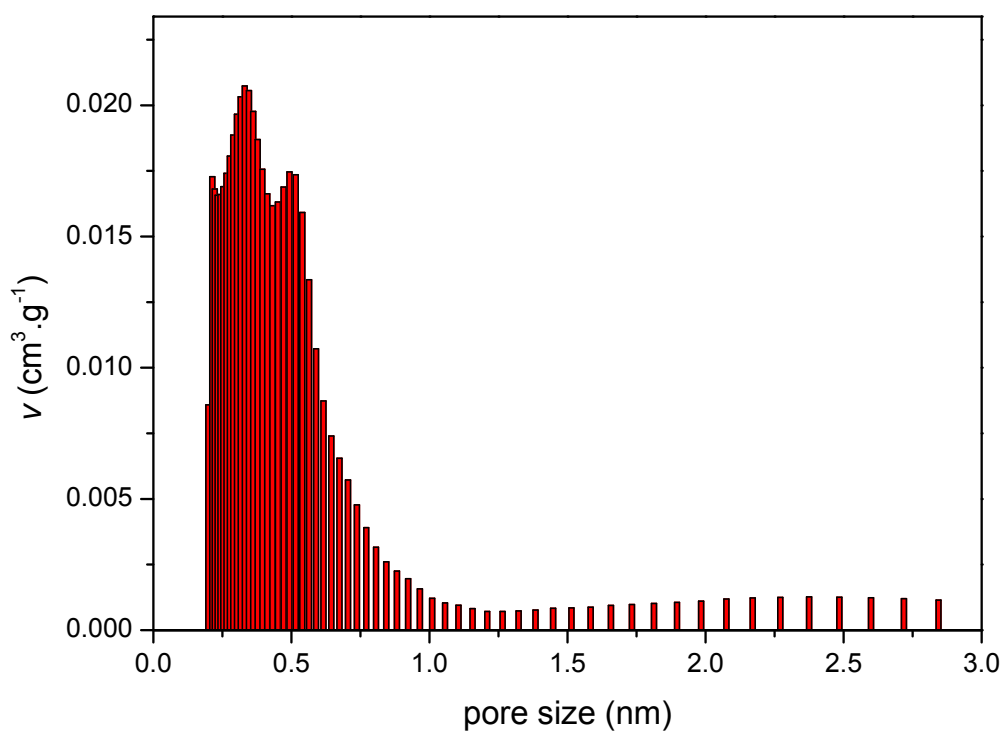


**Figure S12.** DFT pore size distribution of MOF-74.

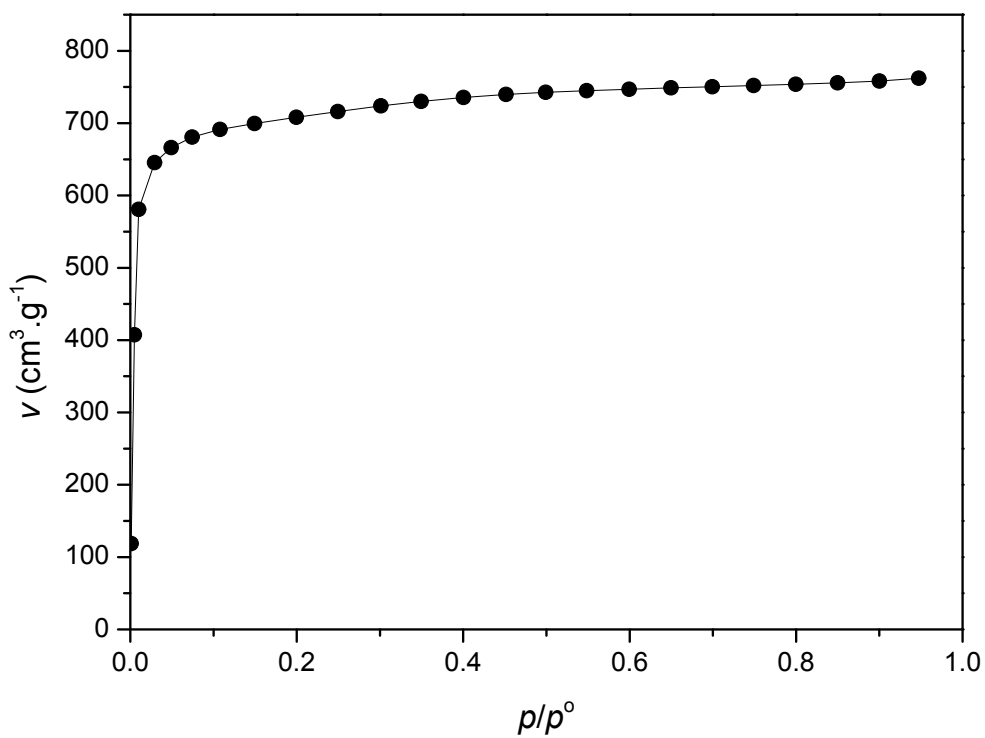


**Figure S13.**  $\text{N}_2$  isotherm of MOF-5 at 77K.

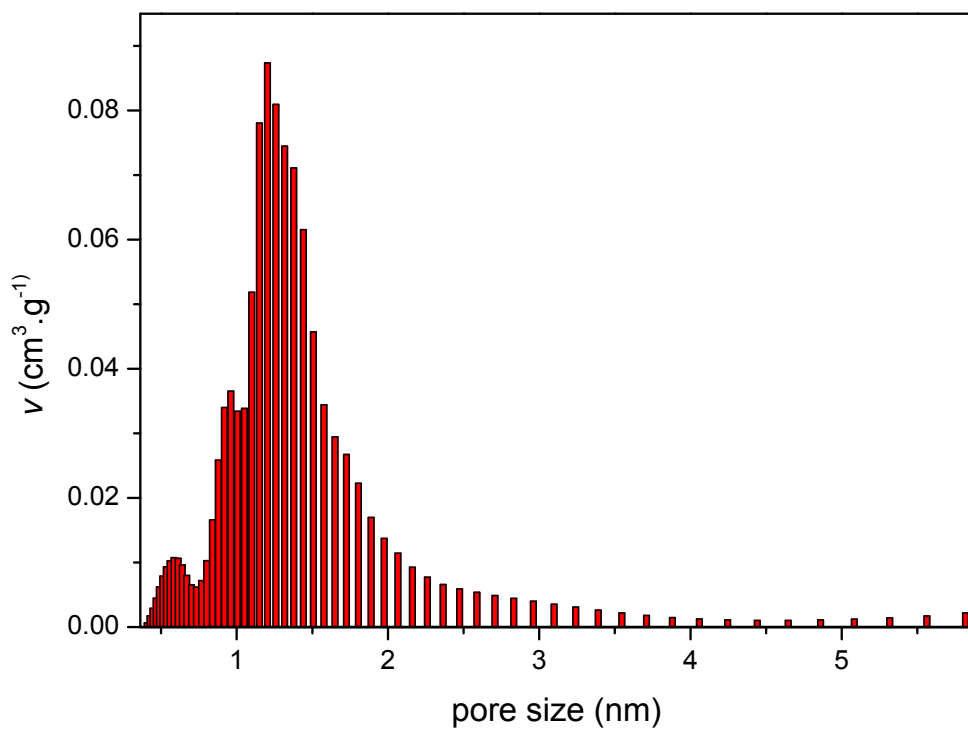


**Figure S14.** DFT pore size distribution of MOF-5.

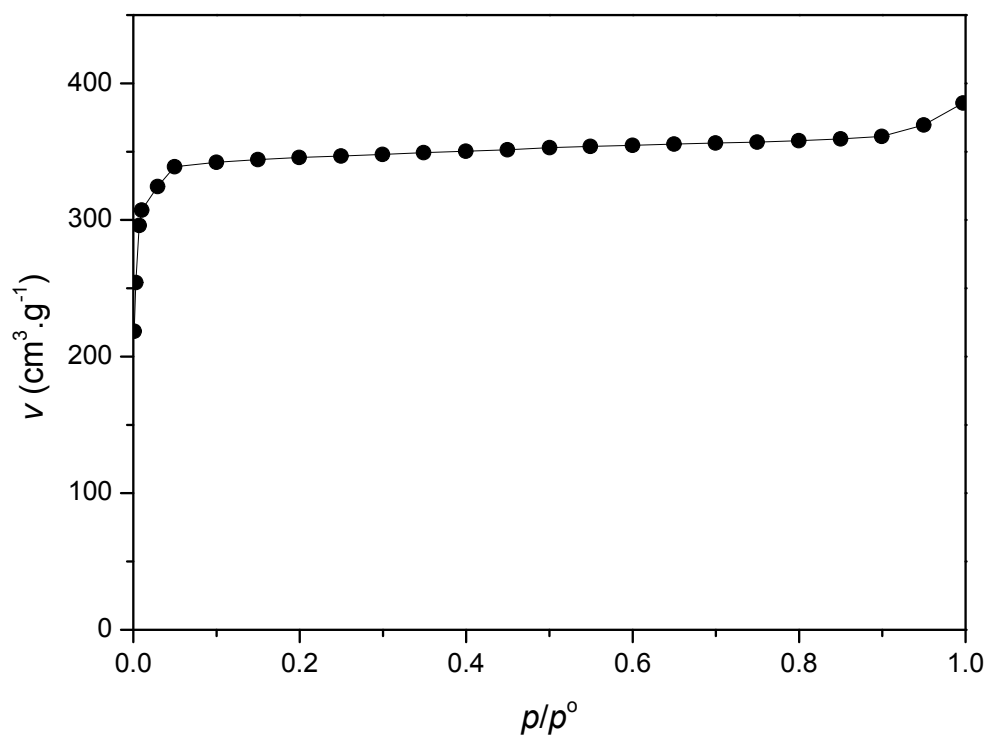


**Figure S15.**  $\text{N}_2$  isotherm of ZIF-8 at 77K.

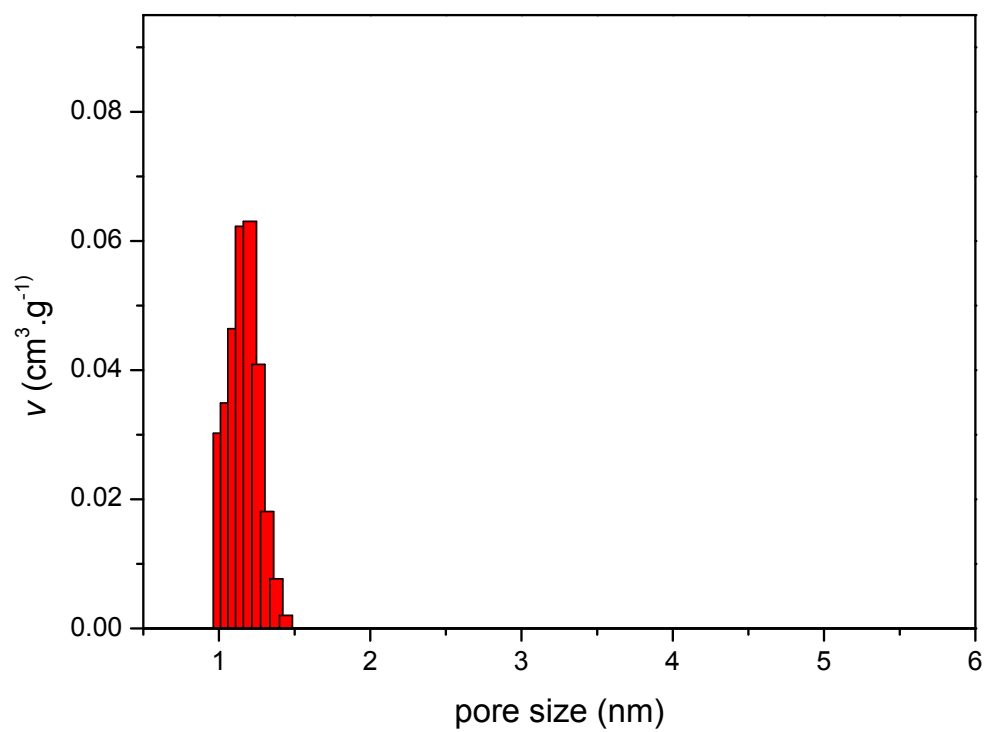


**Figure S16.** DFT pore size distribution of ZIF-8.

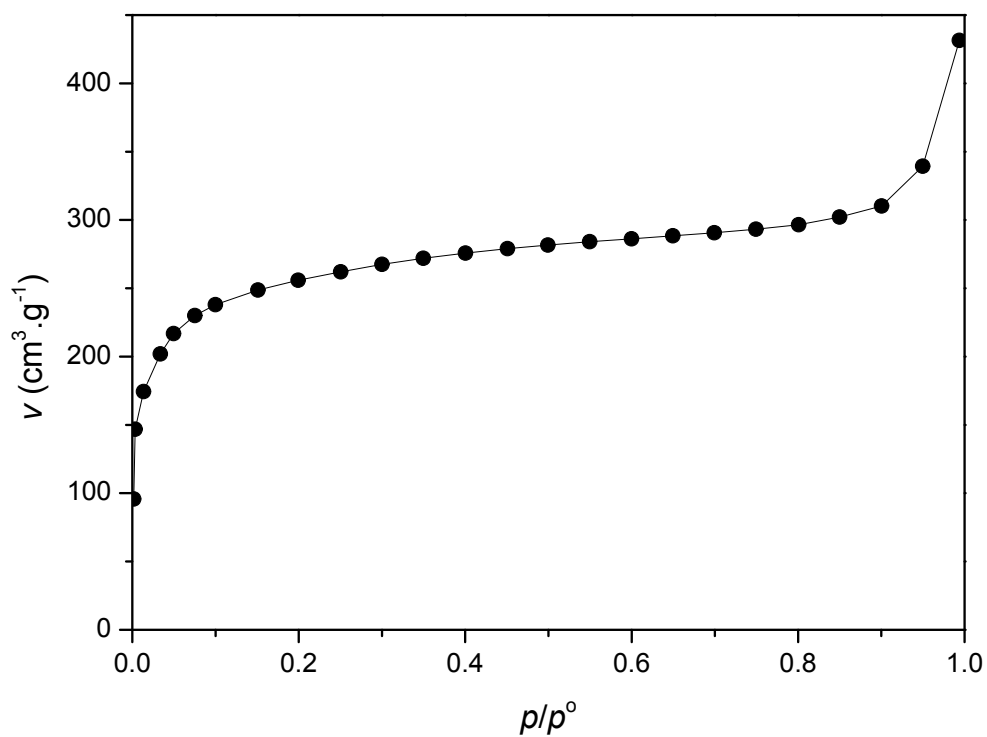


**Figure S17.**  $\text{N}_2$  isotherm of MIL-100(Fe) at 77K.

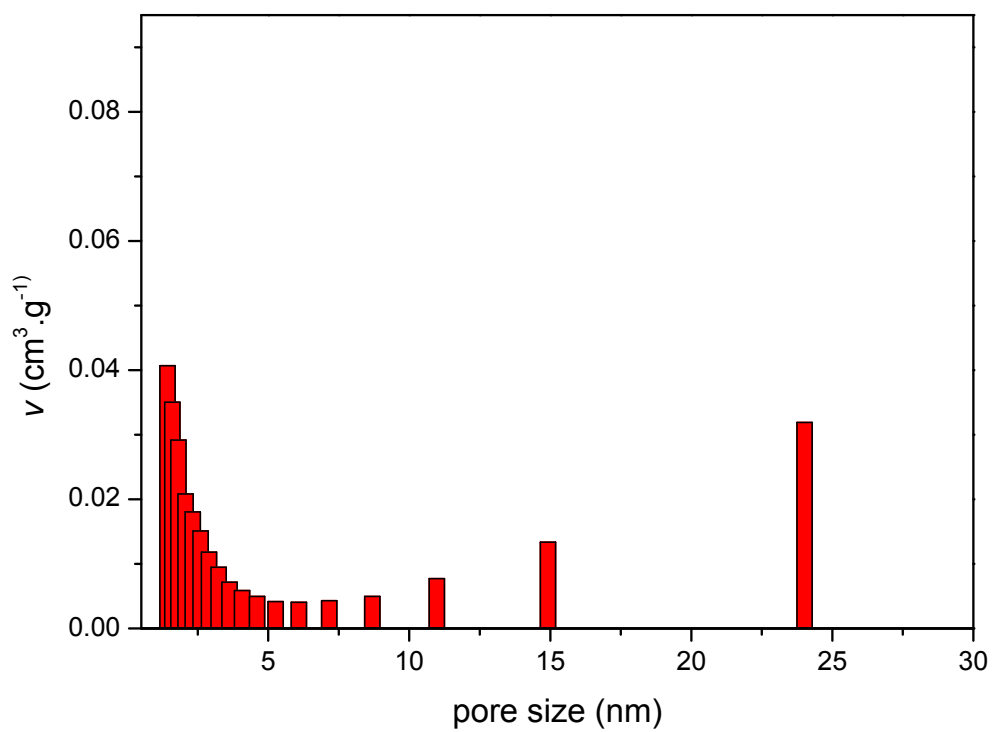


**Figure S18.** DFT pore size distribution of MIL-100(Fe).

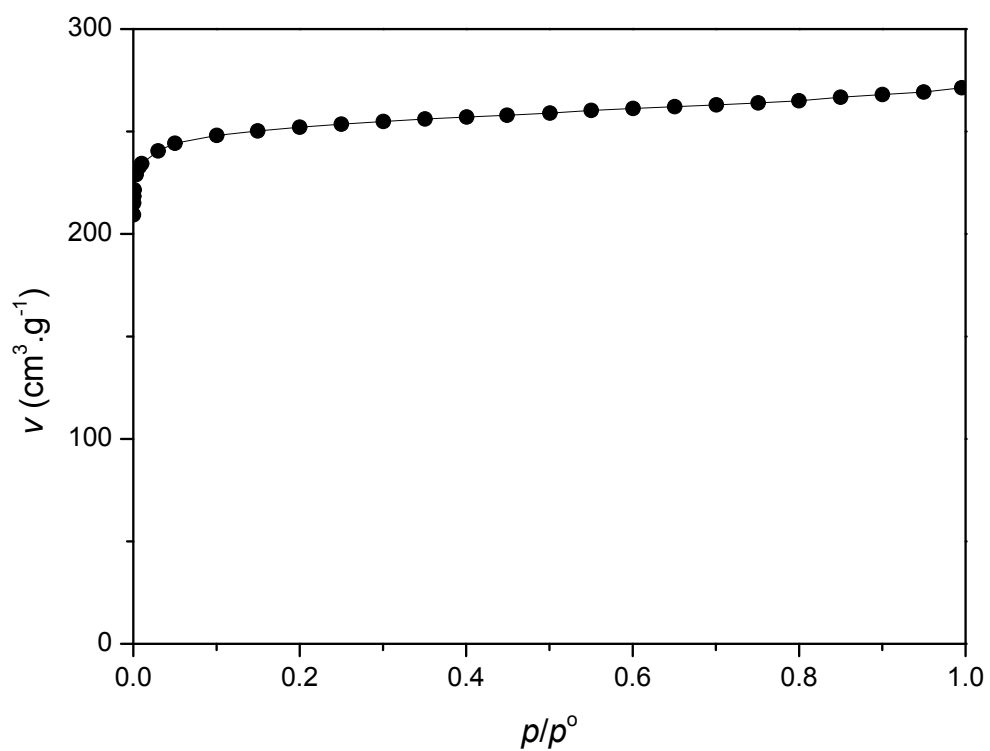


**Figure S19.** N<sub>2</sub> isotherm of Y-BTC at 77K.

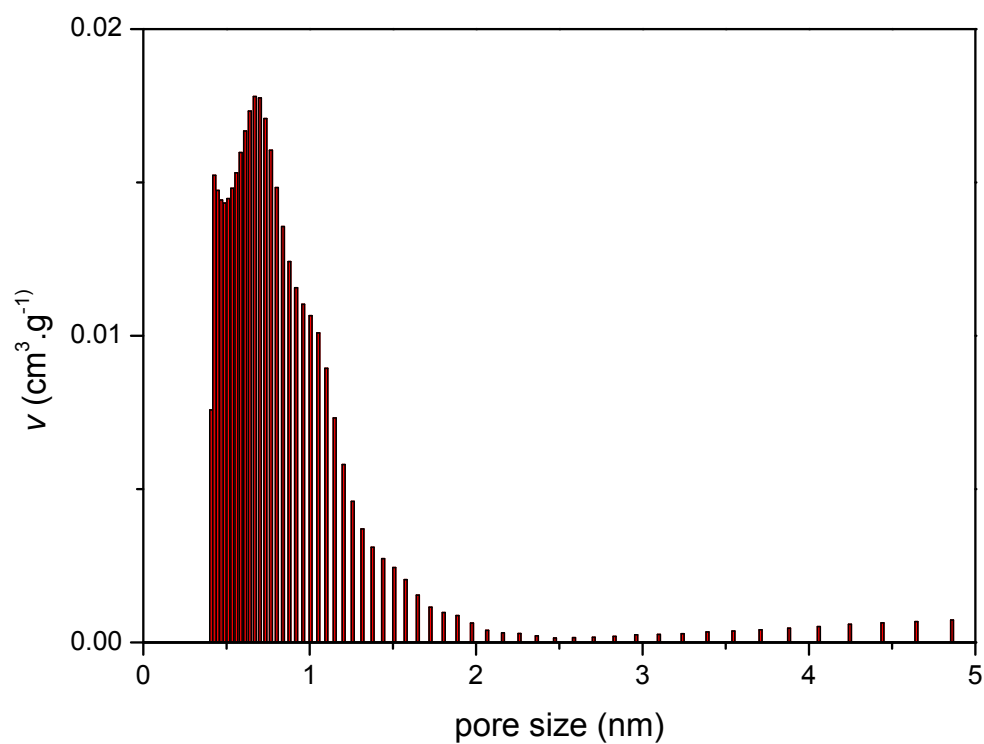


**Figure S20.** DFT pore size distribution of Y-BTC.

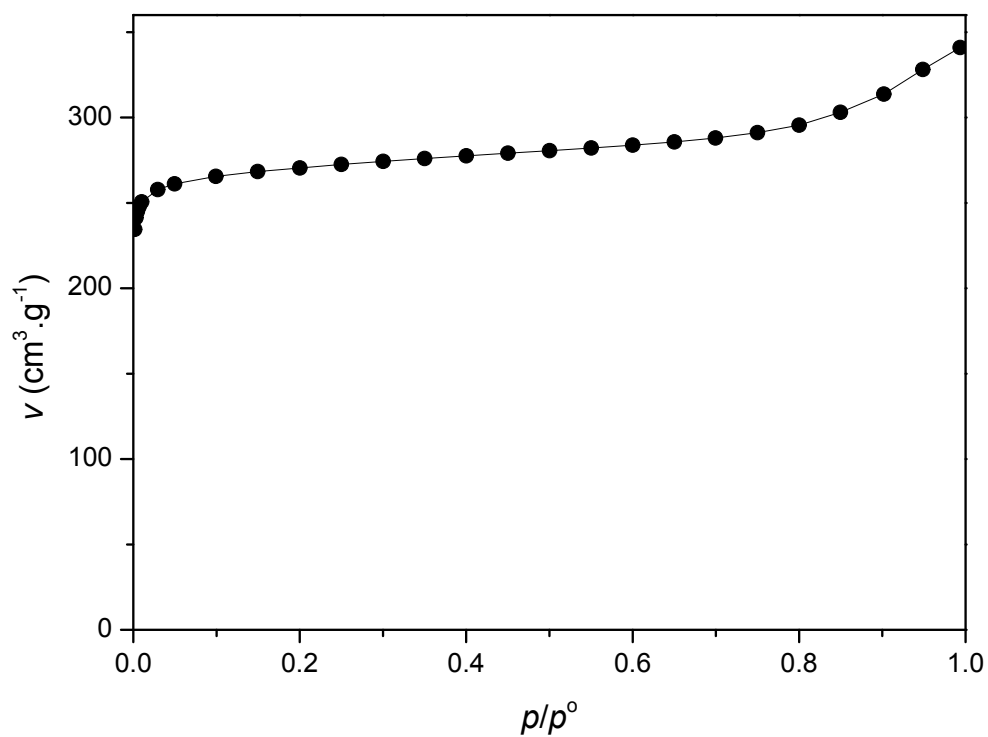


**Figure S21.**  $\text{N}_2$  isotherm of Cu-BTC at 77K.

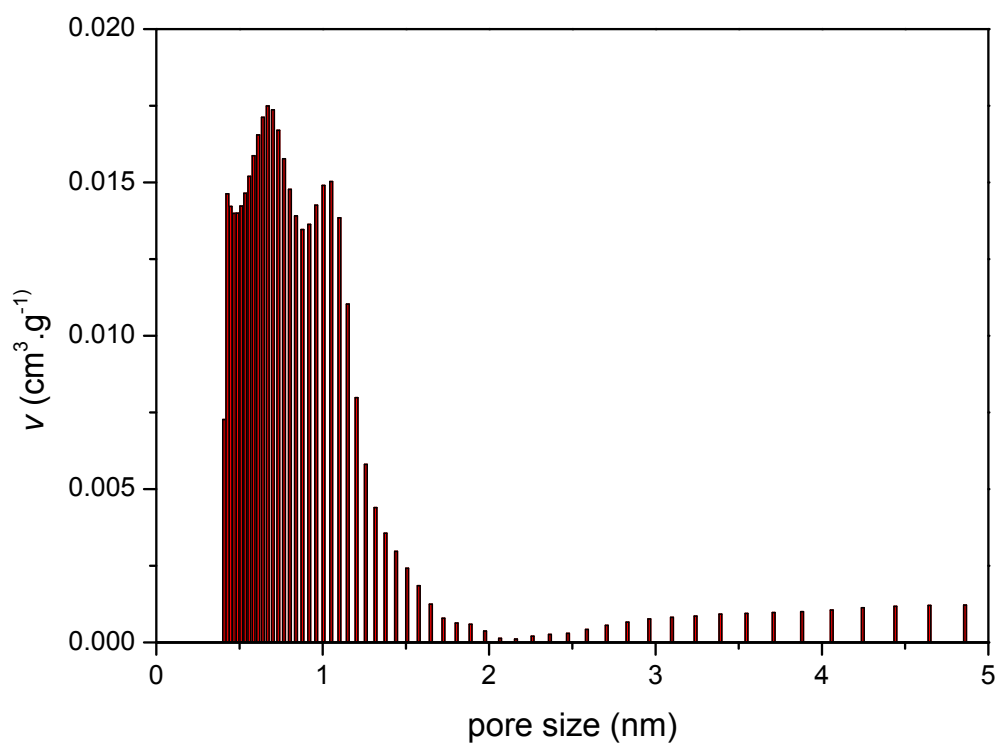


**Figure S22.** DFT pore size distribution of Cu-BTC.



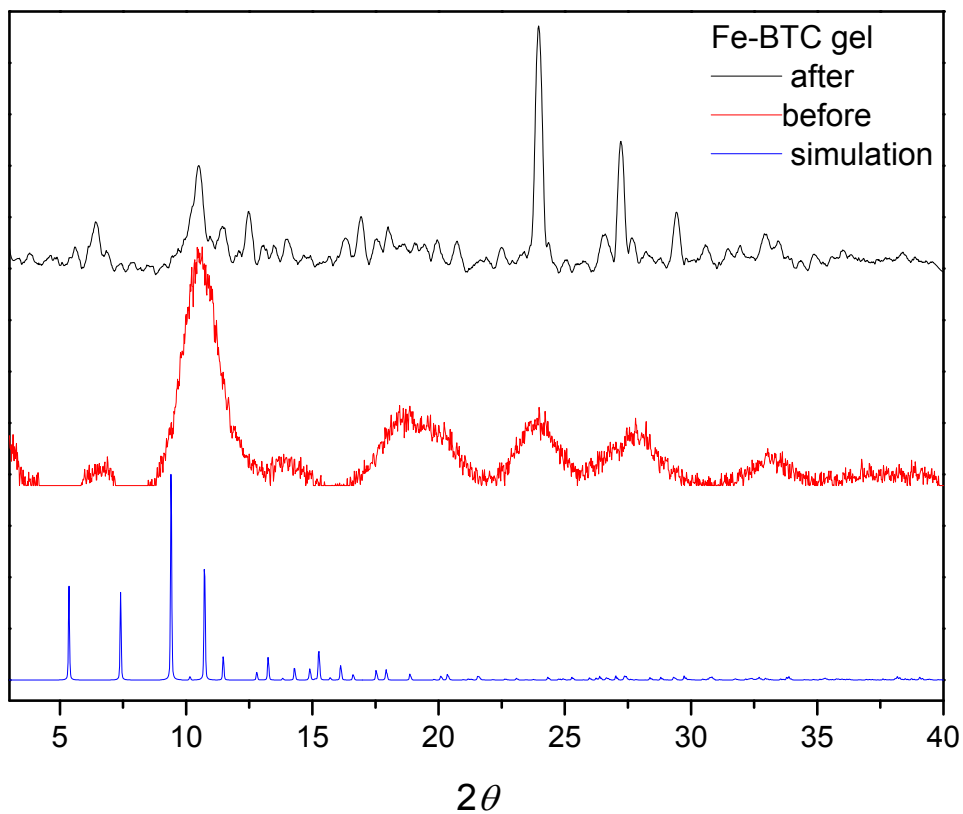


**Figure S23.** PXRD pattern of Fe-BTC gel before and after adsorption of HCl.

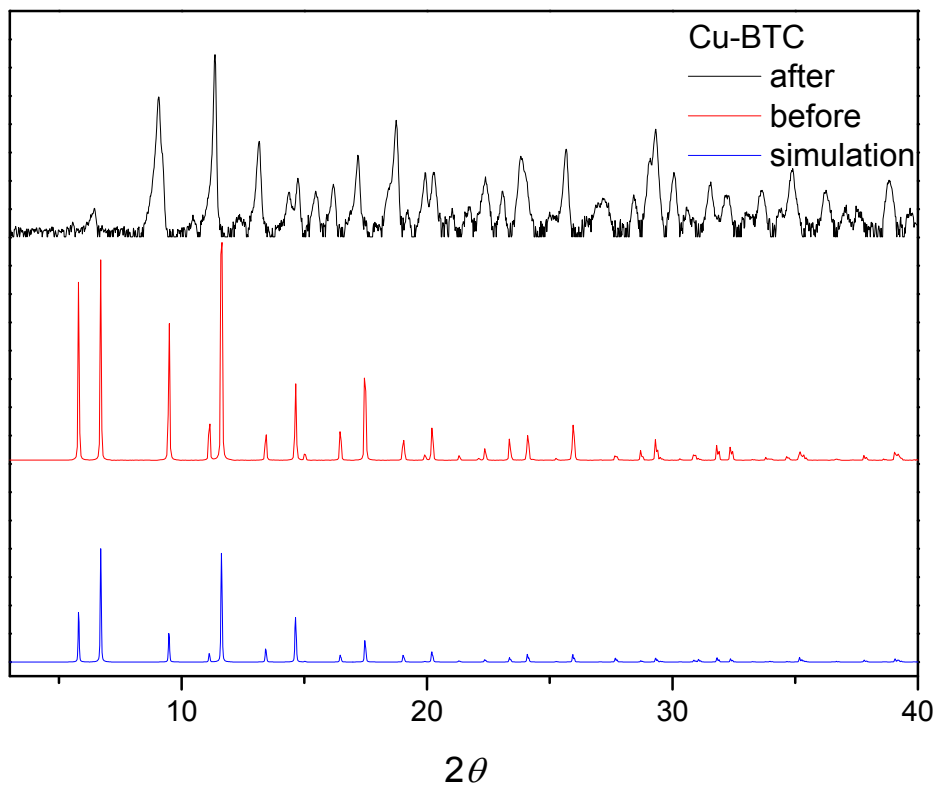


**Figure S24.** PXRD pattern of Cu-BTC before and after adsorption of HCl.

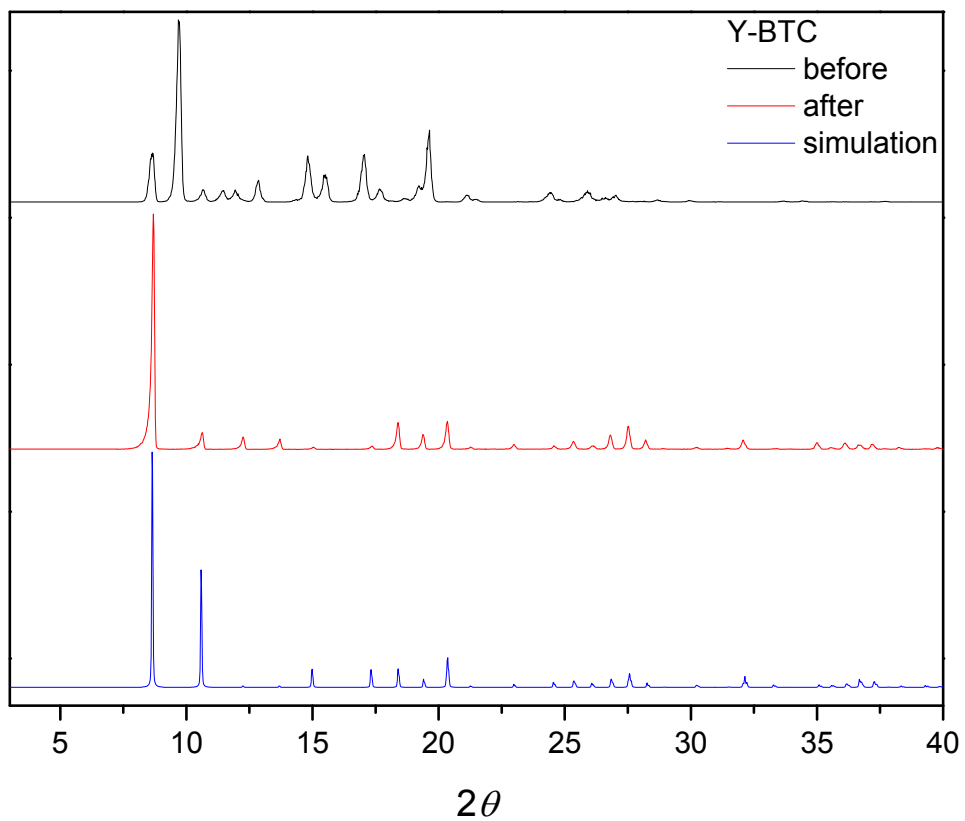


**Figure S25.** PXRD pattern of Y-BTC before and after adsorption of HCl.

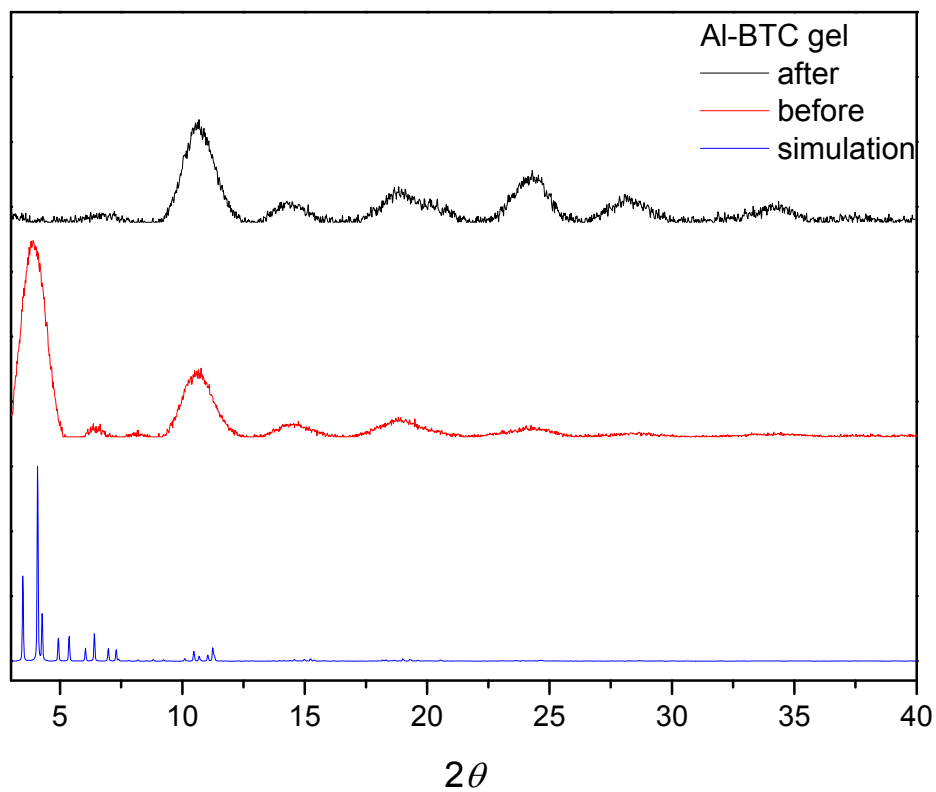


**Figure S26.** PXRD pattern of Al-BTC gel before and after adsorption of HCl.

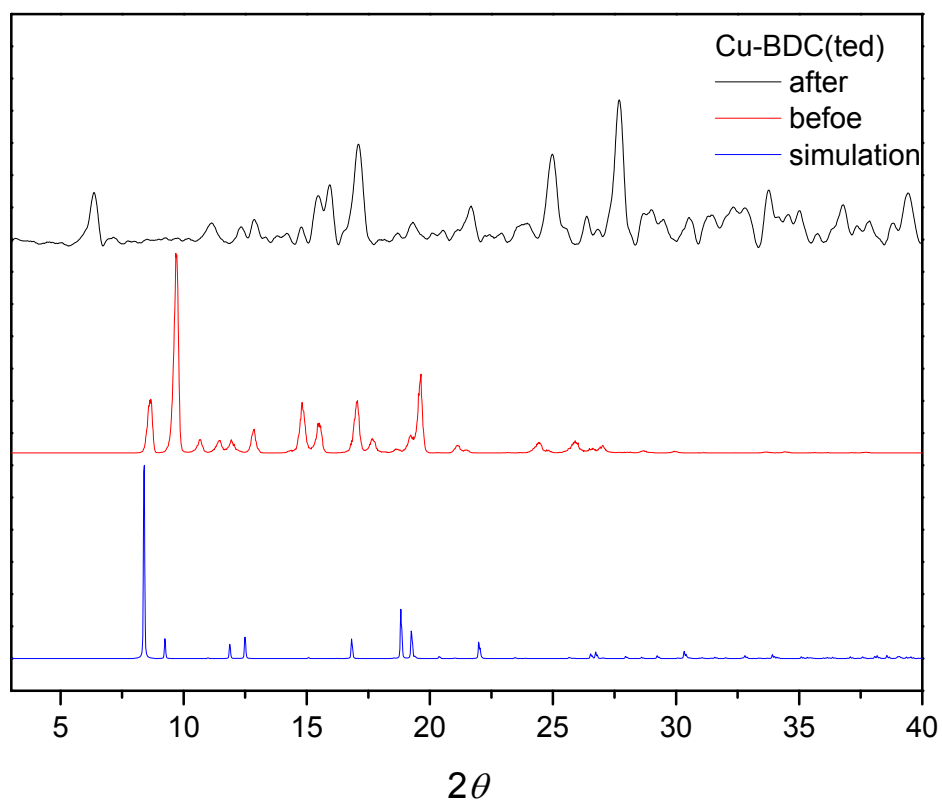


**Figure S27.** PXRD pattern of Cu-BTC(TED) before and after adsorption of HCl.

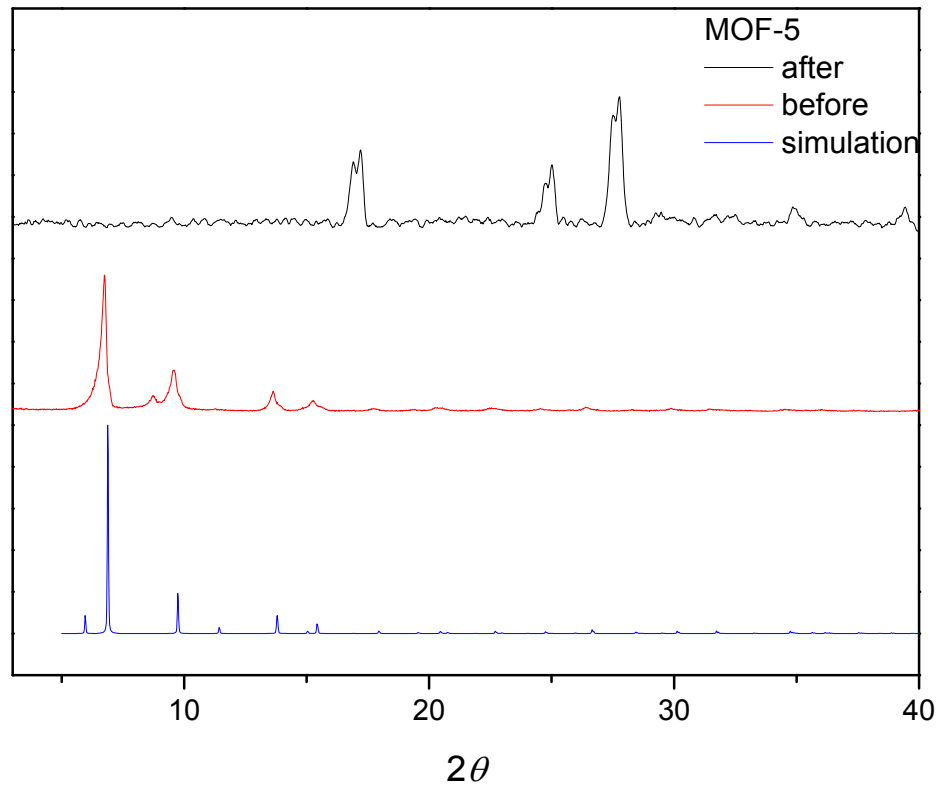


**Figure S28.** PXRD pattern of MOF-5 before and after adsorption of HCl.

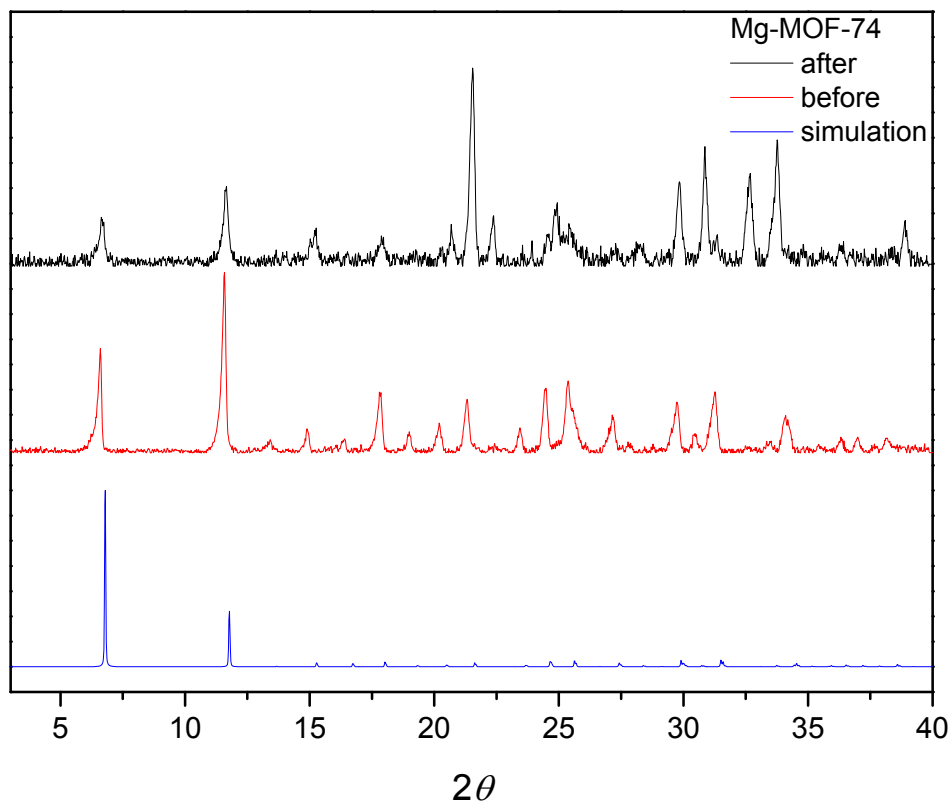


**Figure S29.** PXRD pattern of Mg MOF-74 before and after adsorption of HCl.

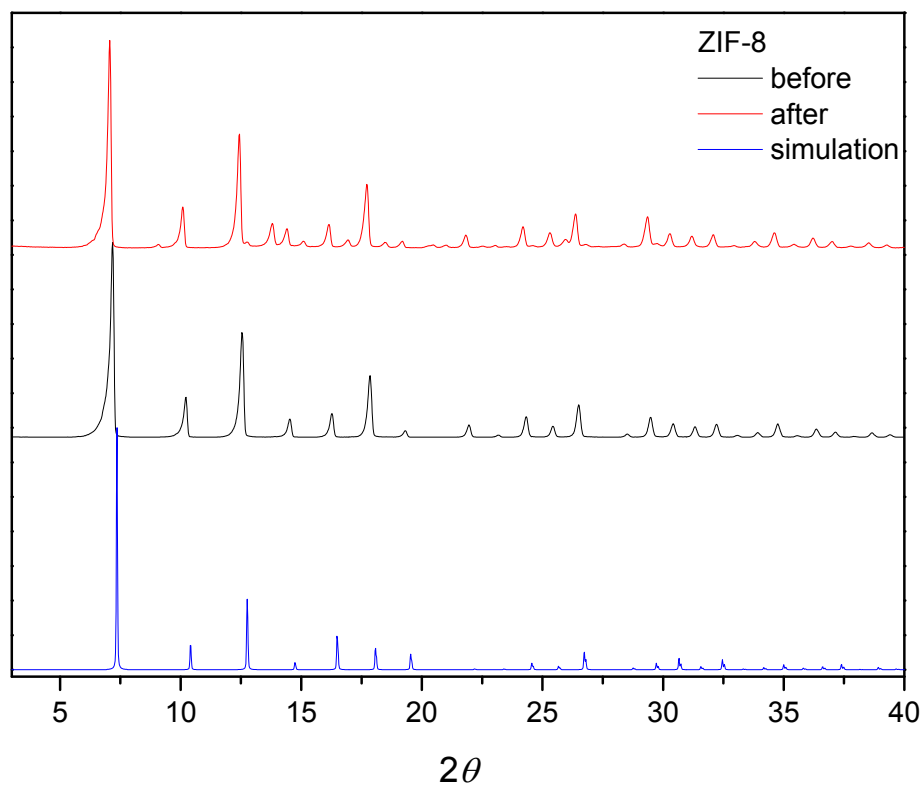


**Figure S30.** PXRD pattern of ZIF-8 before and after adsorption of HCl.

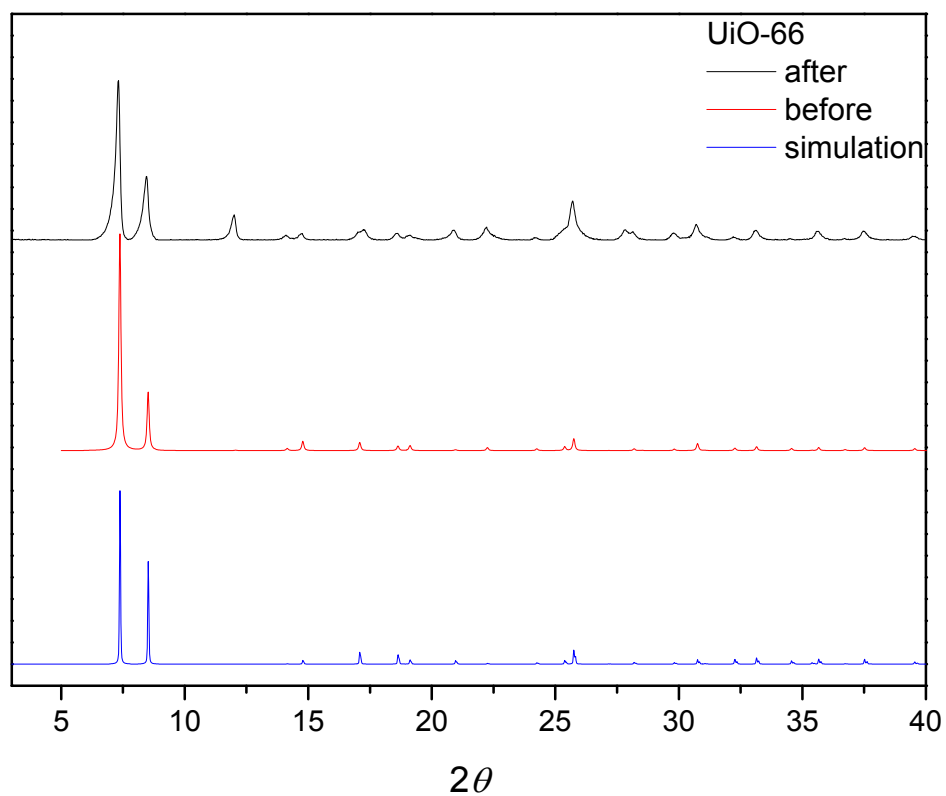


**Figure S31.** PXRD pattern of UiO-66 before and after adsorption of HCl.

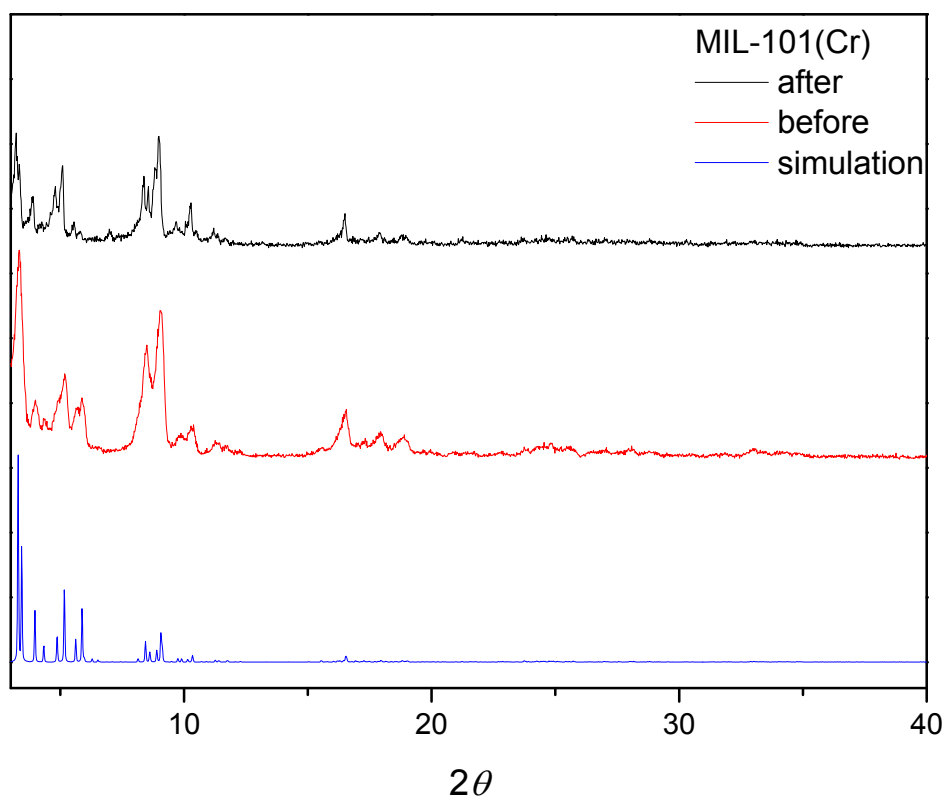


**Figure S32.** PXRD pattern of MIL-101(Cr) before and after adsorption of HCl.

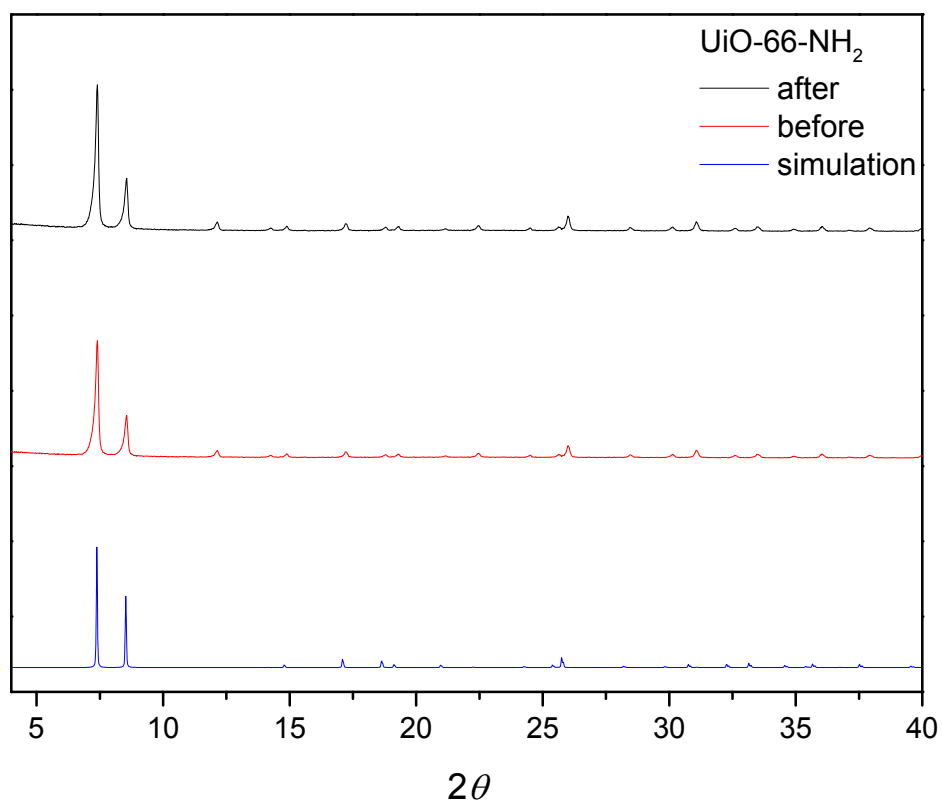


Figure S33. PXRD pattern of UiO-66(NH<sub>2</sub>) before and after adsorption of HCl.

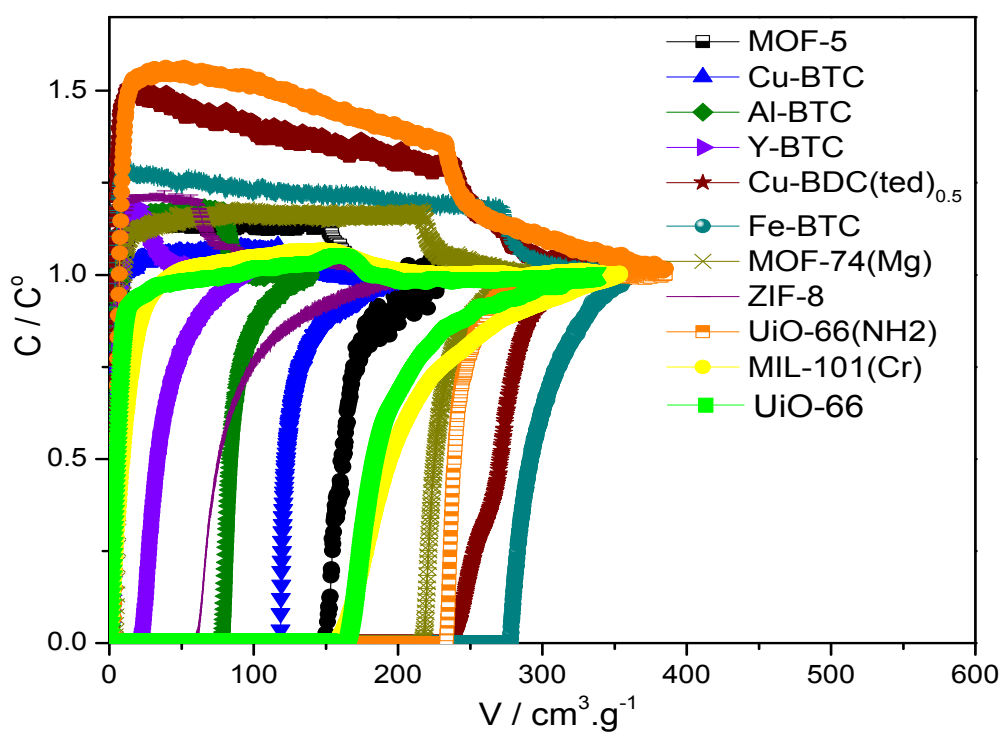


Figure S34. HCl breakthrough on MOFs at 298K.

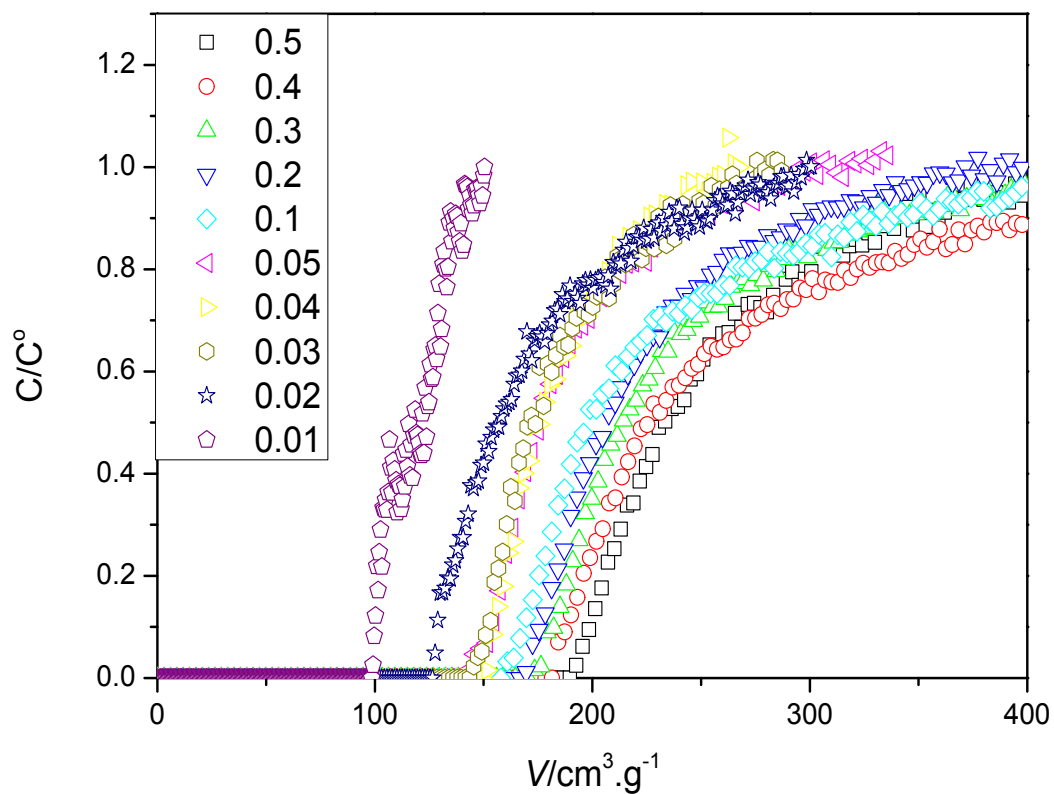


Figure S35. HCl breakthrough on MIL-01(Cr) at 298K at different pressure (bar).

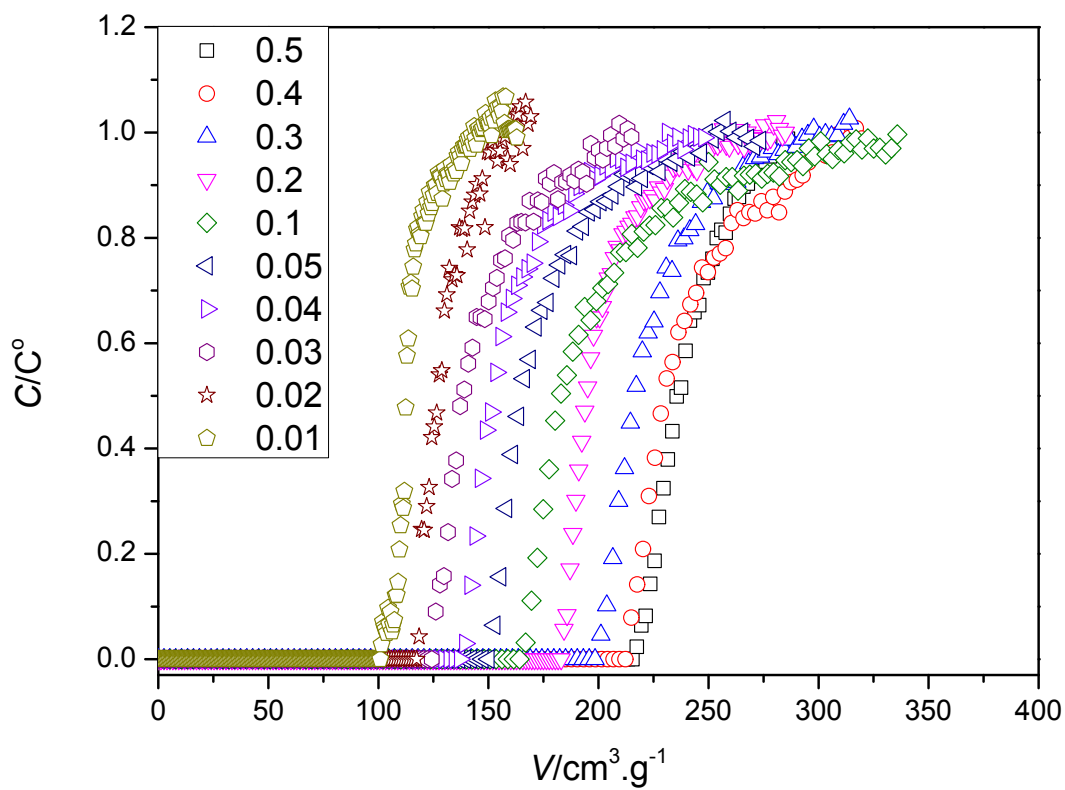
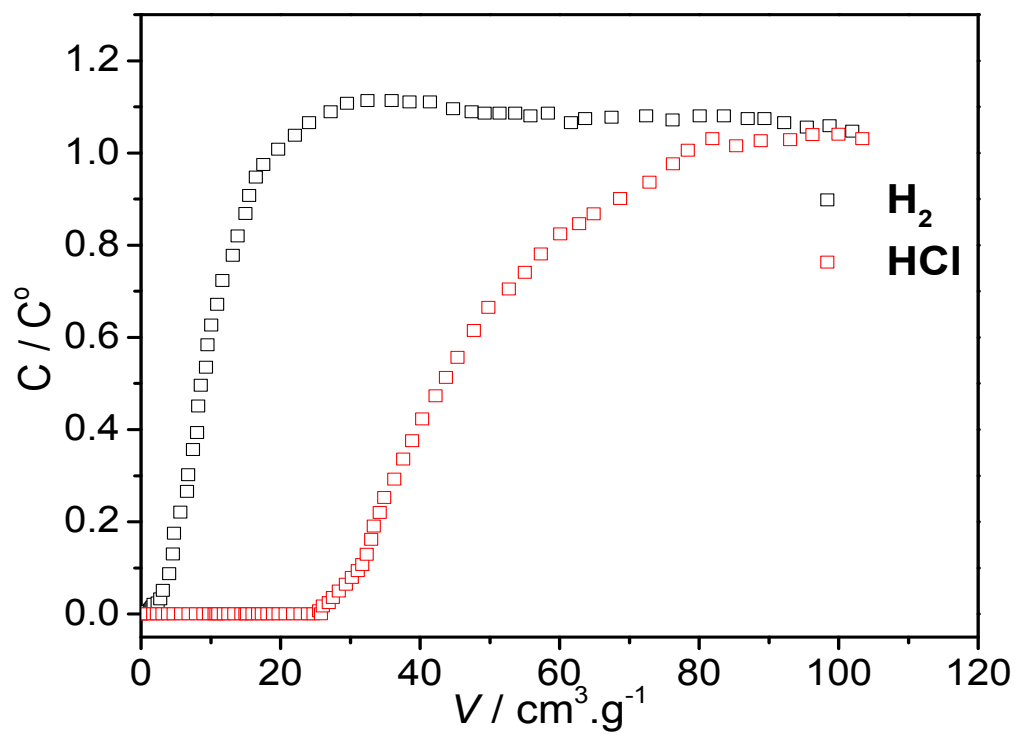


Figure S36. HCl breakthrough on UiO-66 at 298K at different pressure (bar).



**Figure S37.** HCl breakthrough on commercial activated carbon at 1 bar and 298 K.